Photoneutron Cross Sections*

R. Montalbetti, L. Katz, and J. Goldemberg†

University of Saskatchewan, Saskatoon, Saskatchewan, Canada

(Received February 17, 1953)

The neutron yields resulting from photoneutron reactions have been measured as a function of betatron energy from threshold to 23 Mev for 22 elements. These yield curves have been analyzed by the photon difference method to give the total cross section $\sigma = (\sigma_{\gamma,n} + \sigma_{\gamma,np} + 2\sigma_{\gamma,2n})$ as a function of photon energy. Whenever possible, this cross section has been resolved into its components using threshold considerations and subsidiary data. Some general conclusions based on the new results are presented regarding the systematics of (γ, n) reactions.

THE study of photoneutron reactions through the detection of the emitted neutrons offers a number of advantages over the usual residual activity method which have been fully appreciated by workers in this field for a long time. For example, in the case of residual activity some of the nuclei resulting from (γ, n) reactions are stable, others have very long half-lives or decay schemes which have not as yet been determined. This is particularly true in the case of $(\gamma, 2n)$ reactions where the product nuclei, except for the light elements, are long lived, emit soft radiation which is difficult to detect, and have decay schemes which are in the main not known. A disadvantage of the neutron detection method is that it only gives the sum of the (γ, n), $(\gamma, 2n)$ and (γ, np) cross sections.[1] However, when the (γ, n) cross section is known from residual activity the other cross sections may be readily obtained by subtraction.[2] Usually threshold considerations are of great assistance in sorting out these cross sections.

The earliest survey of neutron yields from a large number of elements using a betatron was carried out by Price and Kerst.[3] They measured these yields at only two betatron energies, 18 and 22 Mev, using rhodium foil detectors.

Terwilliger[4] and Jones[5] measured the photoneutron cross sections of eleven elements, using the x-rays from synchrotrons, and detecting the emitted neutrons with BF_3 "long counters." Terwilliger's results cover an energy range of 13.5 to 70 Mev, while the measurements of Jones extend from 80 to 320 Mev. Although both of these experiments suffer somewhat from lack of precise energy control of their bremsstrahlung beams and from low intensity in the 20-Mev region, nevertheless they have contributed greatly to our knowledge of

the photonuclear cross sections at energies above 30 Mev. Recently, Halpern, Nathans, and Mann[6] have reported the photoneutron cross sections for tantalum and bismuth using a method which detected the emitted neutrons. This was accomplished by thermalizing the emitted neutrons in the vicinity of a BF_3 counter which was surrounded by a paraffin cylinder. The scaler was gated so that only those counts occurring some microseconds after each x-ray burst were registered.

In this paper we report on the photoneutron cross sections of some 22 elements covering the periodic table. These measurements extend from threshold up to an energy of 23 Mev; sufficient to include the giant photoabsorption resonance, characteristic of all high-energy photonuclear reactions. The method which we used is similar to that of Halpern et al. The authors would like to thank Dr. J. Halpern for making the design details of his apparatus available to us while his work was still in its initial stages. A complete report of this apparatus has been published by Halpern et al.[7]

EXPERIMENTAL TECHNIQUE

Although a BF_3 counter will detect neutrons efficiently, its energy sensitivity follows the $1/v$ law. In photoneutron reactions the energy of the emitted neutrons range from thermal energies to the order of 10 Mev, depending on the nuclear excitation. As a result it is necessary to make the neutron detector equally
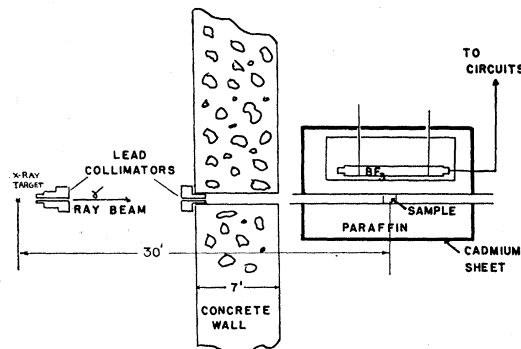
* Based on part on a thesis presented for the Ph.D. degree at the University of Saskatchewan by R. Montalbetti.

† On leave of absence from Departamento de Fisica, Universidade de São Paulo, São Paulo, Brazil.

[1] Other neutron emitting cross section are energetically forbidden in the energy region covered in this experiment.

[2] J. Goldemberg and L. Katz, [Phys. Rev. 89, 1300 (1953)] discuss the validity of such subtractions.

[3] G. A. Price and D. W. Kerst, Phys. Rev. 77, 806 (1950).

[4] K. M. Terwilliger, Ph.D. thesis, University of California Radiation Laboratory Report UCRL-1917, Aug. 1952 (unpublished).

[5] L. Jones, Ph.D. thesis, University of California Radiation Laboratory Report UCRL-1916, Aug. 1952 (unpublished).

Fig. 1. Experimental arrangement.

[6] Halpern, Nathans, and Mann, Phys. Rev. 88, 679 (1952).

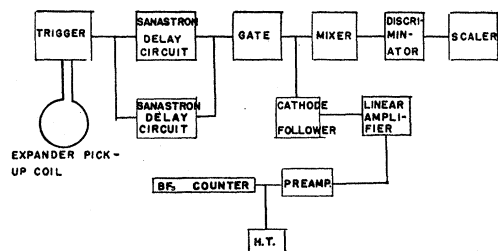[7] Halpern, Mann, and Nathans, Rev. Sci. Instr. 23, 678 (1952).

FIG. 2. Block diagram of electronic system.

efficient at all energies. This was accomplished by embedding the BF_3 counter in a paraffin cylinder. The cylinder also served the purpose of confining the neutrons and thermalizing them in the vicinity of the counter. Figure 1 shows the experimental arrangement. The tank was constructed so that the BF_3 counter could be moved up and down in a slot. This slot was necessary in order to determine a position for the counter which gave equal efficiency of counting for all neutron energies. The method of determining this position will be discussed later.

As will be seen from Fig. 1 the sample was placed inside a 1-in. hole at the center of the paraffin block. The x-ray beam which was highly collimated was allowed to strike the sample without hitting any other material.

In order to obtain good counting statistics it was necessary to reduce the neutron background to a very low value. The large neutron flux which accompanied the x-ray burst is sufficient to cause piling-up of counts. These neutrons arise mainly from (γ, n) reactions in the betatron target and the lead shield. It was found that with the equipment in the betatron room, shielded by 8 in. of concrete and approximately 2 ft of water the background was still too high to make an accurate determination of the activation curves.

A solution to this problem was to move the BF_3 detector outside the building where a 7-ft concrete wall could be utilized to considerably reduce this background. The neutrons which did pass through the wall possessed only thermal energies and were captured by the cadmium sheet surrounding the paraffin tank.

A 2-in. hole was drilled through the wall and a lead collimator was inserted. The equipment was aligned photographically so that the x-ray beam had a clear path through the paraffin tank.

The counter experiences a large pile-up of secondary electrons during the x-ray pulse. This was eliminated by means of a gated counting circuit. An electronic system was built so that the photoneutrons which were detected could be counted between the x-ray bursts. These x-ray bursts, of some 4 μsec duration, occur 5500 μsec apart. The electronic system contained a gate which opened 20 μsec after this burst and closed again some 800 μsec later. Neutron pulses were registered on a scaler during the time that this gate is open. Figure 2

shows the electronic system in block diagram. The expander pulse was delayed by two delay circuits which opened and closed a gate at the desired times. The neutron pulses were amplified and fed into a mixer along with the gate signal. The resulting signal was then fed into a discriminator which discriminated the neutron pulses from background.

It was found that by increasing the time beyond 800 μsec gave no appreciable increase in neutron counts. Also by shortening the initial dead time the background rose in greater proportion than the neutron counts so that the values of 20 μsec and 800 μsec were optimum settings.

Samples to be irradiated were placed inside the paraffin tank. It was determined experimentally that for over a region of 10 cm on either side of the center of the BF_3 counter the counting rate remained constant. Beyond this region the counting rate decreased rapidly. Care was taken to locate the samples within this constant counting rate region.

TABLE I. Relative magnitude of background to neutron counting rate for various samples and betatron energies.

Element	Energy	Neutron count (per 10 monitor clicks)	Background (per 10 monitor clicks)
Na	15.4	210	46
(0.55 mole)	19.0	402	78
	22.2	720	98
Cu	15.4	2657	46
(0.27 mole)	19.0	6848	78
	22.2	10 340	98
Bi	15.4	5198	46
(0.086 mole)	10.0	8233	78
	22.2	9530	98

The amount of irradiation a sample received was measured by a Victoreen chamber placed in a 4-cm Lucite block. The Victoreen was placed some 100 cm from the betatron target and aligned so that it "saw" the same portion on the x-ray beam as that "seen" by the sample. Since the activation curves were to be determined relative to copper it was only necessary to calculate the relative dose received by each of the samples.

The procedure for measuring an activation curve was then straightforward. The background for various betatron energies was initially determined with no sample in place. The sample was then inserted and the number of neutrons emitted for a given dose was counted as a function of the betatron energy.

An example of the magnitude of the background count compared to the neutron count is given in Table I.

It is evident that for elements of medium and heavy atomic weight the counting rate necessary for good counting statistics was many times the background. In the region of the light elements however the cross sec-
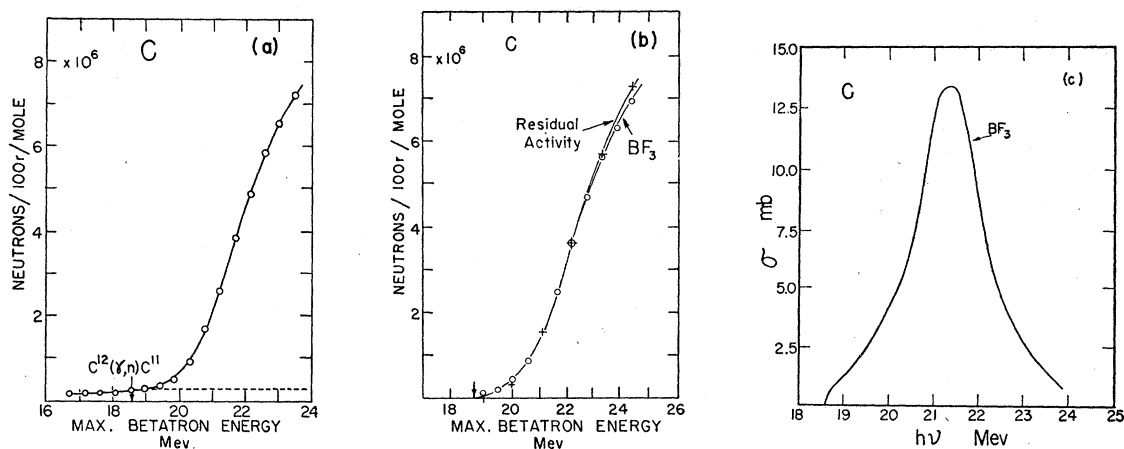
FIG. 3. (a) Neutron yield from a carbon sample as a function of betatron energy. Neutrons below the C^{12} threshold (18.7 Mev) are from the 1.1 percent isotope C^{13} which has a threshold of 4.9 Mev. (b) Neutron yield from $C^{12}(\gamma, n)C^{11}$ reaction as measured by residual activity and direct neutron detection (BF_3) of this experiment. The neutrons from C^{13} shown in Fig. 3(a) have been subtracted. (c) Cross section for the reaction $C^{12}(\gamma, n)C^{11}$ calculated from the neutron yield curve by the photon difference method.

tions are low so that with the size of samples used the neutron counts were only 5 times the background. Nevertheless it was still possible to determine the activation curves quite accurately.

ENERGY SENSITIVITY OF COUNTING SYSTEM

Since calibrated neutron sources were not available to us, it was not possible to determine directly the energy sensitivity of the experimental setup. The method adopted was to compare the shape of the activation curves obtained with the BF_3 counter to that obtained by residual activity, in an element where the (γ, np) and $(\gamma, 2n)$ reactions are energetically forbidden in the energy region examined. One such element available for this comparison is carbon. C^{12} is a 99 percent isotope with thresholds of 28.2 and 32.3 Mev for the (γ, np) and $(\gamma, 2n)$ reactions. Though its activation curve had been previously determined by residual activity,[8] a redetermination was made on the same day as the neutron curve was measured.[9] The position of the BF_3 counter was varied in the slot (Fig. 1) until the activation curve measured by it agreed in shape with that found by residual activity.

As the betatron energy is increased the average nuclear excitation energy increases. This results in an increasing mean energy of the emitted neutrons. The activation curve obtained by residual activity gives a measure of the relative numbers of these neutrons at each betatron energy. Thus when the two activation

curves agree in shape, neutrons of different energy are detected with equal efficiency. The results are shown in Figs. 3(a) and (b).

Natural carbon contains 1.1 percent of C^{13} which has a threshold of 4.9 Mev for the (γ, n) reaction. The neutrons in Fig. 3(a) below the $C^{12}(\gamma, n)$ threshold are from this reaction. It is well known that (γ, n) activation curves level off at about 6 Mev above threshold and remains sensibly constant with increasing betatron energy. For this reason the contribution to the neutron flux from C^{13} may be expected to remain sensibly constant above the C^{12} threshold as indicated by the dashed line. Subtracting this contribution gives the activation curve for the C^{12} isotope, which is shown in Fig. 3(b). The curve obtained by residual activity is shown in the same figure for comparison.

It will be seen that the two curves are in excellent agreement up to 4 Mev above threshold and differ by only 4 percent at 6 Mev from threshold. The neutron distribution for a given nuclear excitation in such a light element as carbon has a much higher mean energy than from heavier nuclei. Thus since good agreement was obtained for carbon, the system may be expected to be energy insensitive up to equivalent excitation energies in the heavier elements.

NORMALIZATION

In order to obtain the absolute neutron yield per unit mass of sample per unit of irradiation it is necessary to calibrate our apparatus. The procedure usually followed in this laboratory is to use the (γ, n) reaction in copper as a standard. The absolute cross section for this reaction in both isotopes of copper had been previously measured in this laboratory by residual activity.[10] The cross section for the Cu^{63} isotope has been measured

[8] Haslam, Johns, and Horsley, Phys. Rev. 82, 270 (1951).

[9] A very disturbing effect was found in this determination. The new activation curve differed considerably from that measured about 2 years ago. The cross-section curve obtained from it is now somewhat more symmetric and peaks at about 0.8 Mev lower than before (21.3 Mev). This change in activation curve shape will be discussed at greater length in a forthcoming paper by Goldemberg and Katz. Intercomparison of activation curves of the lighter elements taken in different laboratories show similar differences. This will be brought out more clearly in our discussion of phosphorus.

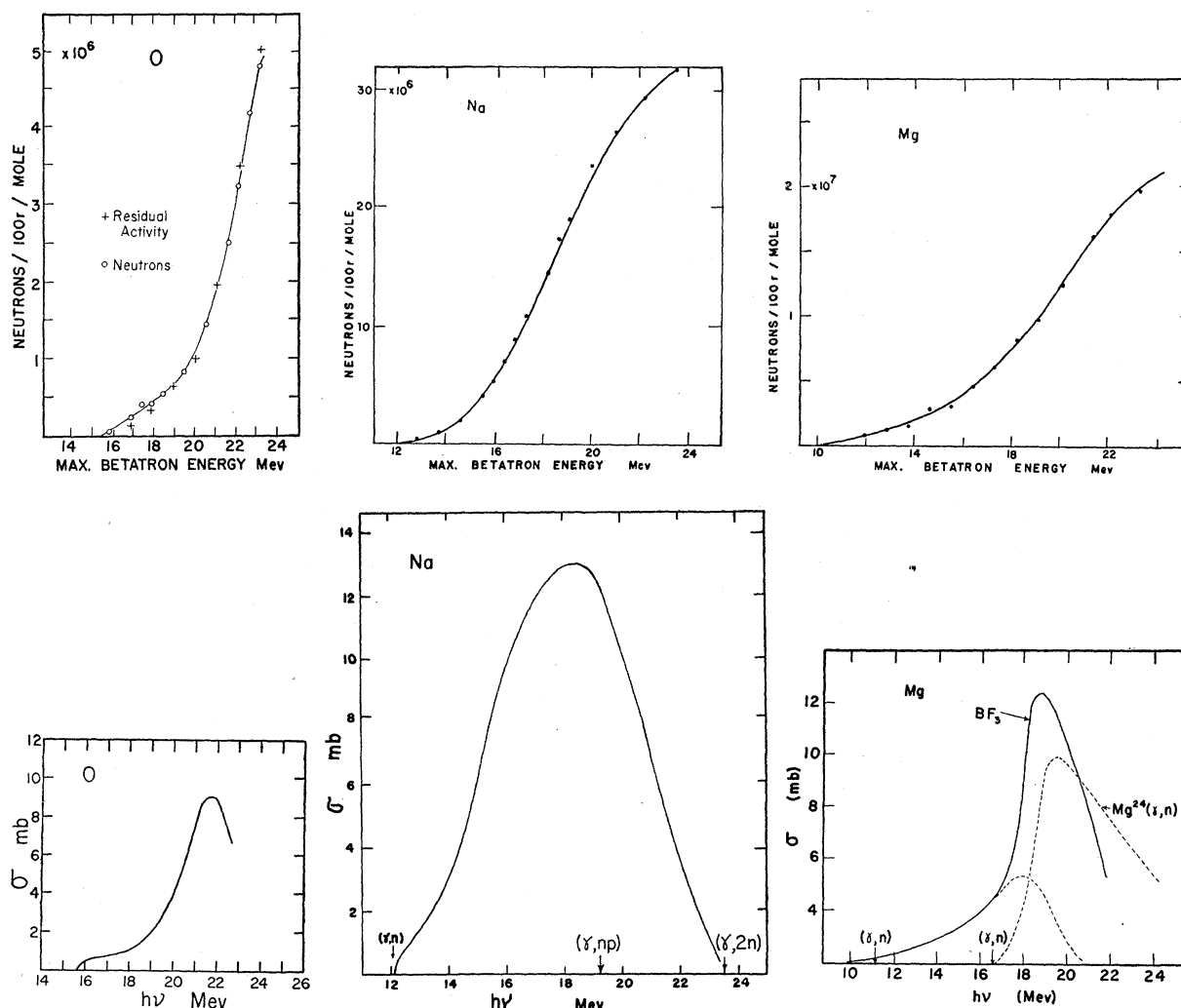[10] Johns, Katz, Douglas, and Haslam, Phys. Rev. 80, 1602 (1950).

FIG. 4. Neutron yields from the indicated elements as measured by direct detection of the emitted neutrons, and the cross sections calculated from them by the photon difference method. See the more detailed discussion in the contents of the article.

independently in a number of laboratories[11-13] and our value has been well substantiated. The cross section for the Cu[65] isotope has been measured independently by Byerly and Stephens[12] and is in good agreement with our value. Combining these two cross sections according to the isotopic abundance of Cu[63] and Cu[65], the (γ, n) cross section for the natural element was obtained. The neutron yield for each element in our experiment was compared to that of copper with the betatron energy set at 18 Mev. This allowed us to calculate the absolute neutron yield for these elements at this energy.

The shapes of the yield curves were obtained in a series of experiment extending over a period of five weeks. All curves were then calibrated against copper in one continuous run. The betatron was kept at 18-

Mev, samples of the various elements were irradiated one after the other, and the resulting neutron yields were measured. To assure that the energy of the betatron and the sensitivity of the apparatus remained constant, the yield from an aluminum sample was checked periodically.

The normalization point was chosen at 18 Mev since no $(\gamma, 2n)$ is present in copper at this energy. The threshold for $C^{12}(\gamma, n)C^{11}$ is 18.6 Mev and for this reason carbon was normalized against copper at 21 Mev.

Many of the photons which are "absorbed" in the sample only suffer Compton scattering and therefore have a second chance to produce photoneutron reactions, though they have been assumed to be lost in our calculations below. Calculations show that for the size of samples used in this experiment at most 2 percent of all photoneutrons at 24-Mev irradiation could be attributed to this effect.

[11] B. C. Diven and G. M. Almy, Phys. Rev. 80, 407 (1950).
[12] P. R. Byerly and W. E. Stephens, Phys. Rev. 83, 54 (1951).
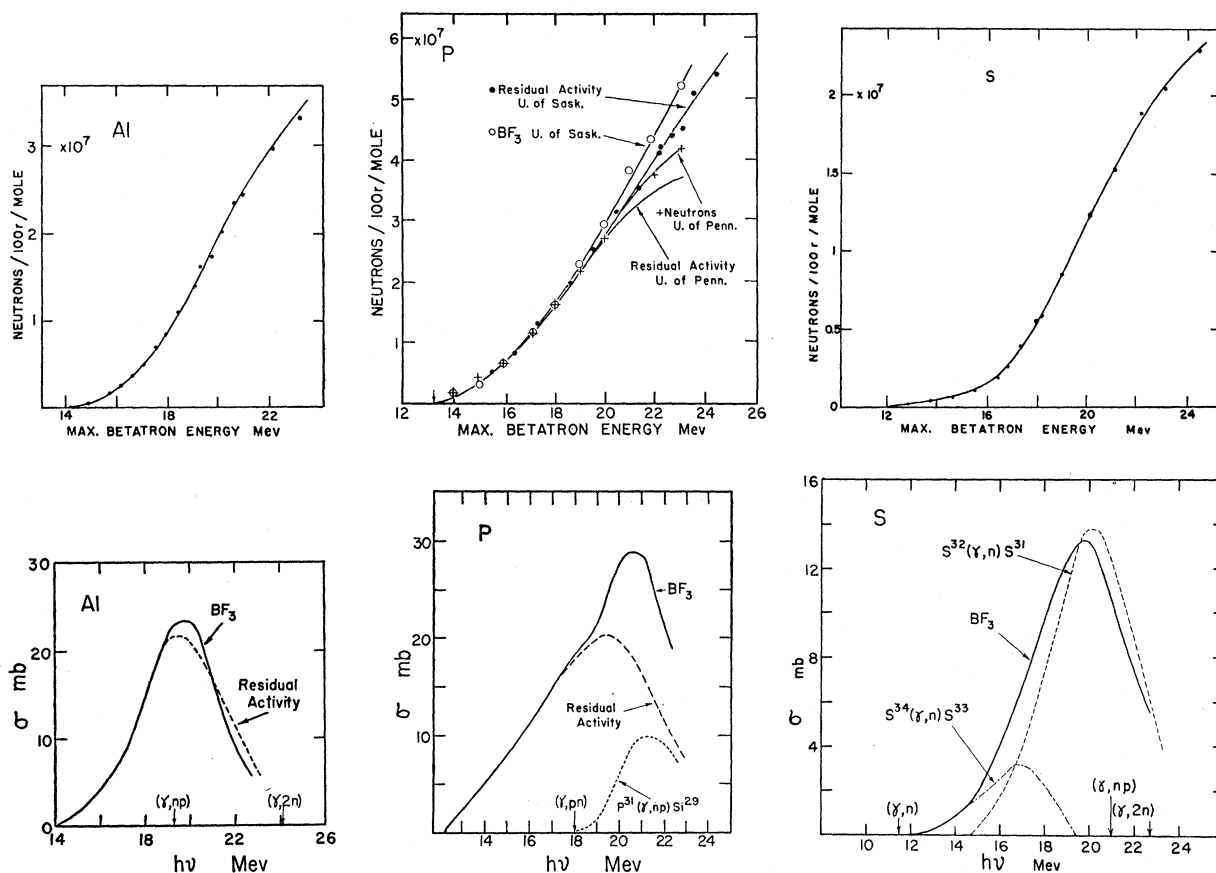[13] V. E. Krohn, Jr., and E. F. Shrader, Phys. Rev. 87, 685 (1952).

FIG. 5. Neutron yields from the indicated elements as measured by direct detection of the emitted neutrons, and the cross sections calculated from them by the photon difference method. See the more detailed discussion in the contents of the article.

RESULTS

The yield curves which were obtained are shown in Figs. 4 to 10. Before these curves can be analyzed for the photoneutron cross sections, it is necessary to correct for absorption of the bremsstrahlung beam in the sample itself. Small samples are usually used in the residual activity experiments so that this correction is negligible. However, in order to obtain sufficient neutron flux in our experiment with the apparatus situated some 30 feet from the betatron target, considerably larger samples had to be used. This correction is no longer negligible and was applied as follows:

Consider a sample of length l, density ρ and cross-sectional area a, then if α' is the activity from the sample, the activity per mole is:

$$\alpha = \alpha' A / \rho a l.$$

Thus

$$\frac{\alpha' A}{\rho a l} = N \int_0^{E_0} \sigma(E) P(E, E_0) dE \int_0^l \frac{e^{-\mu \rho x}}{l} dx,$$

where $\sigma(E)$ is the cross section for the reaction; $P(E, E_0)$ is the number of photons per cm^2 per 100r/min per Mev interval of energy E when betatron is operating

at an energy E_0, μ is the total absorption coefficient in units of cm^2/g, and N is Avogadro's number.

Integration with respect to x gives

$$\alpha = N \int_0^{E_0} \sigma(E) P(E, E_0) \left[\frac{1 - e^{-\mu \rho l}}{\mu \rho l} \right] dE.$$

The variation with energy of the bracketed term was calculated for the size of samples used. The variation was found to be 1 percent over an energy region of 10 Mev to 22 Mev. For this reason the bracketed term may be taken outside of the integral and the following equation is obtained:

$$N \int_0^{E_0} \sigma(E) P(E, E_0) dE = \frac{\alpha' A \mu}{a(1 - e^{-\mu \rho l})}.$$

It is seen from this last equation that after the observed activity is corrected for sample size and photon absorption the basic equation for the photon difference method is obtained. This correction has been applied to the activation curves which are shown in Figs. 3(b) and 4 through 10. These curves were analyzed by the photon difference method and the resulting cross sec-
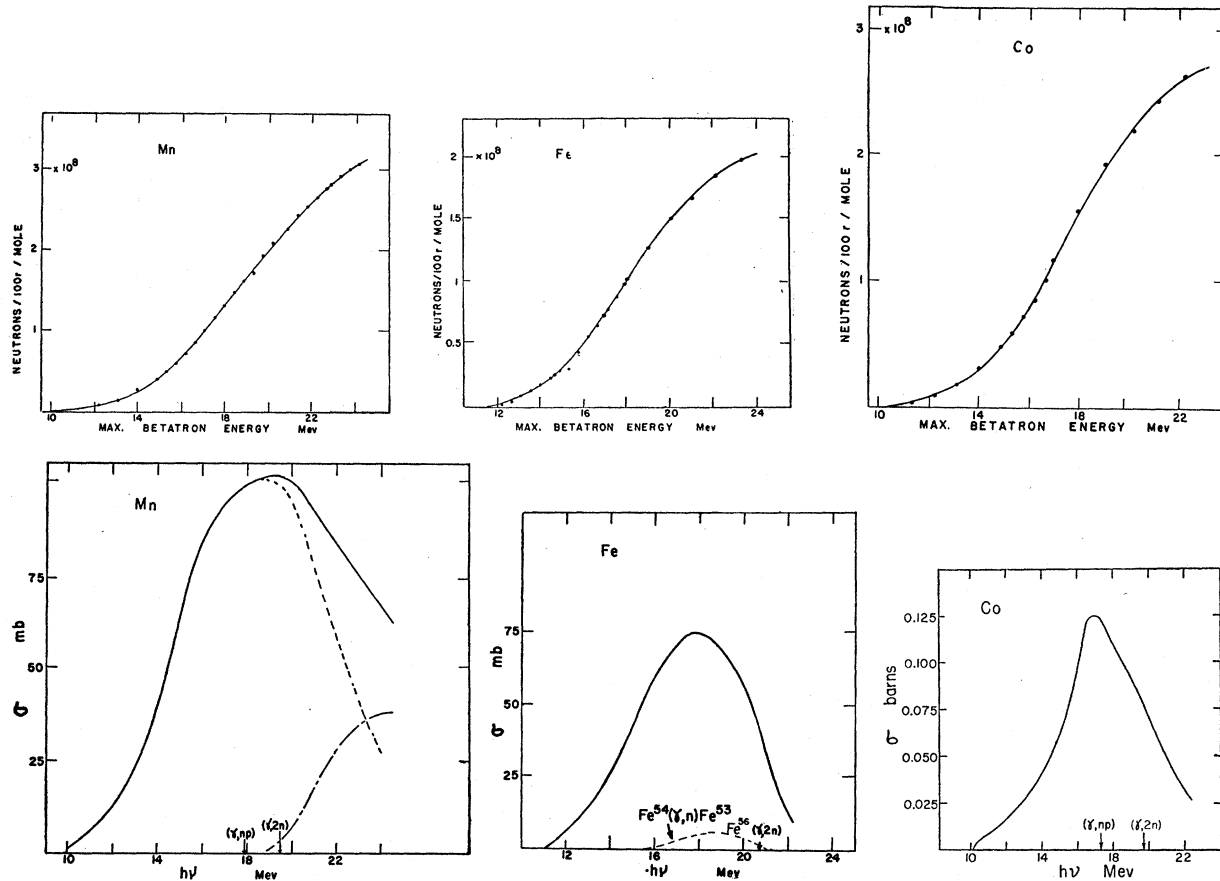
FIG. 6. Neutron yields from the indicated elements as measured by direct detection of the emitted neutrons, and the cross sections calculated from them by the photon difference method. See the more detailed discussion in the contents of the article.

tions[14] are shown in Figs. 3(c) and 4 through 10. As many of the 100 percent isotopes as possible were measured. In these cases the determination of the $(\gamma, 2n)$ contribution is of course much easier to evaluate than when there are several large percentage isotopes present.

The (γ, np) and $(\gamma, 2n)$ thresholds are indicated on the individual cross section curves. These were calculated from mass data whenever those were available. In the lighter elements the data of Li et al.[15] and Li[16] were used, the masses of some of the heavier elements were kindly supplied by Duckworth[17] or were taken from the literature.[18] When no mass data were available the thresholds were calculated from the table of atomic masses by Metropolis and Reitwiesner.[19] The (γ, n) thresholds of our activation curves were in good agreement with those published by Sher, Halpern, and

Mann.[20] They are not given explicitly since no effort was made to determine them accurately.

The pertinent data obtained for each element have been collected together and are presented in Table II. Previous measurements obtained predominantly by the residual activity method are also given in this table. Each of the curves will now be discussed separately. Heading each of the discussions is a list of the isotopes in the element, their abundance and the (γ, n) threshold (Mev) in each. These data are necessary for a proper interpretation of each of the curves.

Carbon (C^{12} 98.9 Percent, 18.6; C^{13} 1.1 Percent, 4.9)

The cross-section curve obtained by the neutron experiment agrees very well with that obtained using the most recent residual activity measurements. This is of course evident from the excellent agreement between the activation curves. The new curves differ somewhat in shape and area from that found previously in this laboratory by residual activity measurements[8] but the values of the peak cross sections are well within experimental error.

[14] It is to be noted that wherever the cross section includes contributions from the $(\gamma, 2n)$ reaction the cross-section shape is distorted since two neutrons are emitted per absorbed photon.

[15] Li, Whaling, Fowler, and Lauritsen, Phys. Rev. 83, 512 (1951).

[16] C. W. Li, Phys. Rev. 88, 1038 (1952).

[17] H. E. Duckworth (private communication).

[18] R. E. Halsted, Phys. Rev. 88, 666 (1952).

[19] N. Metropolis and G. Reitwiesner, U. S. Atomic Energy Commission Document NP-1980 (unpublished).

[20] Sher, Halpern, and Mann, Phys. Rev. 84, 387 (1951).

FIG. 7. Neutron yields from the indicated elements as measured by direct detection of the emitted neutrons, and the cross sections calculated from them by the photon difference method. See the more detailed discussion in the contents of the article.

Oxygen (O^{16} 99.8 Percent, 15.6; O^{17} 0.04 Percent, 4.2; O^{18} 0.20 Percent, 8.0)

The agreement between the yield curves obtained from residual activity and direct neutron detection offers further proof that the neutron apparatus is equally sensitive to all neutron energies encountered in this experiment.

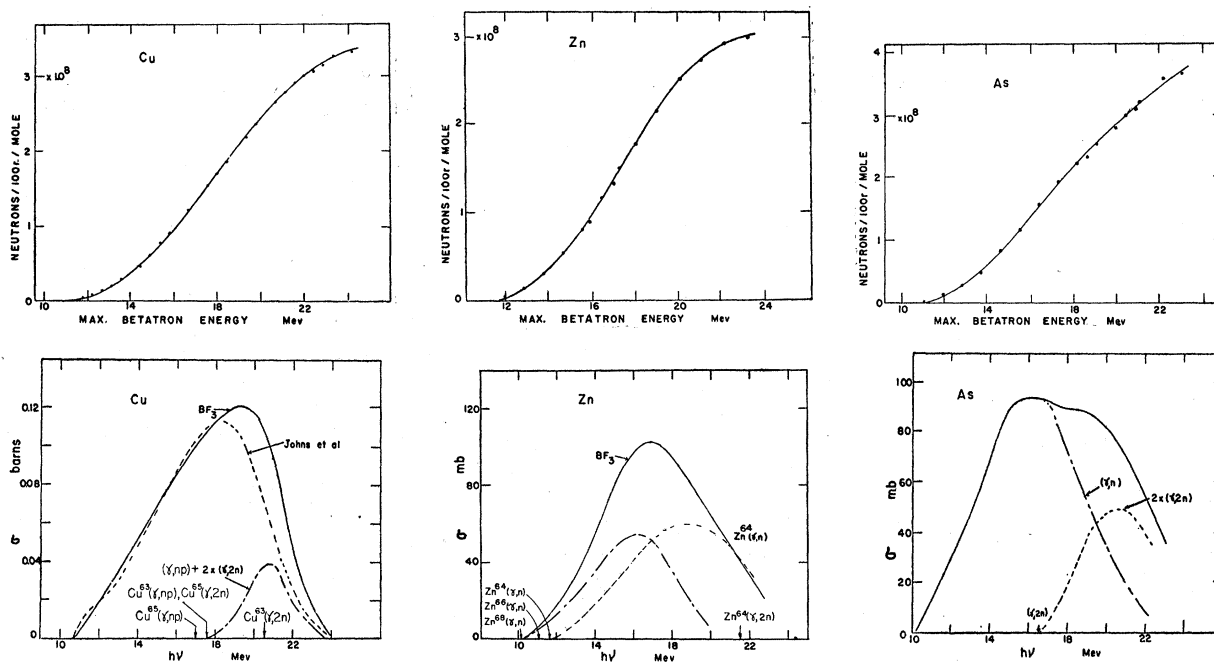The cross-section curve exhibits the initial flat region

FIG. 8. Neutron yields from the indicated elements as measured by direct detection of the emitted neutrons, and the cross sections calculated from them by the photon difference method. See the more detailed discussion in the contents of the article.

FIG. 9. Neutron yields from the indicated elements as measured by direct detection of the emitted neutrons, and the cross sections calculated from them by the photon difference method. See the more detailed discussion in the contents of the article.
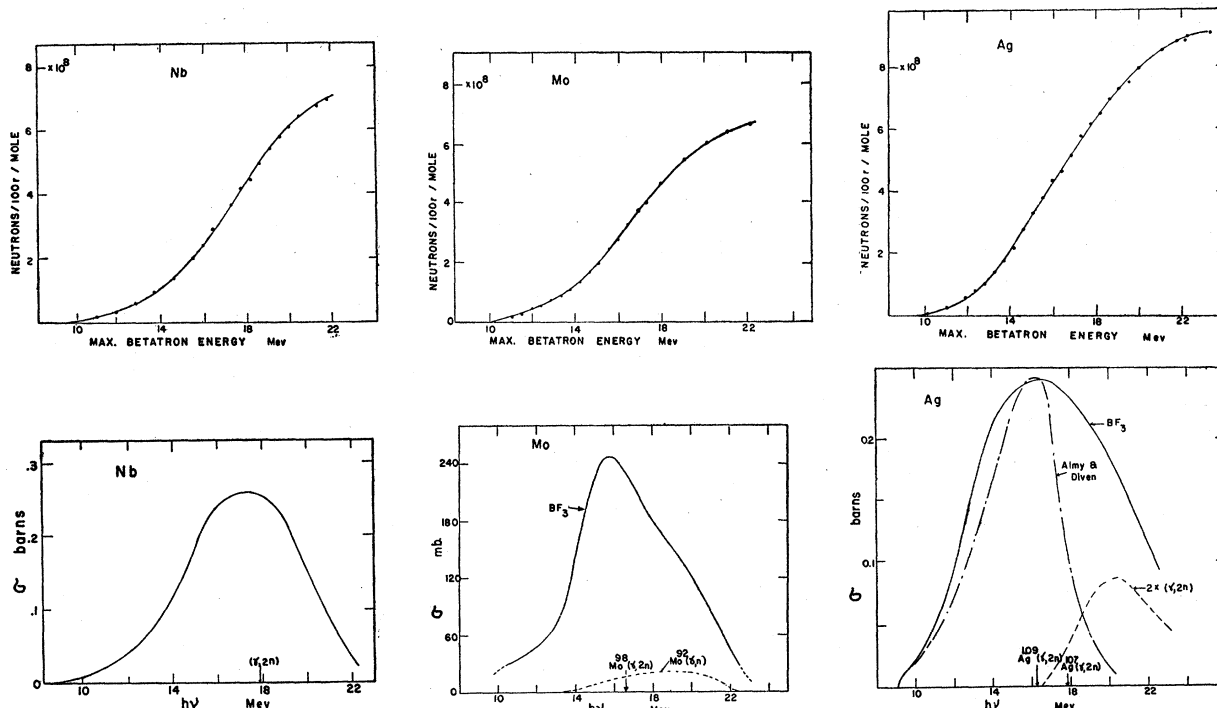

FIG. 10. Neutron yields from the indicated elements as measured by direct detection of the emitted neutrons, and the cross sections calculated from them by the photon difference method. See the more detailed discussion in the contents of the article.
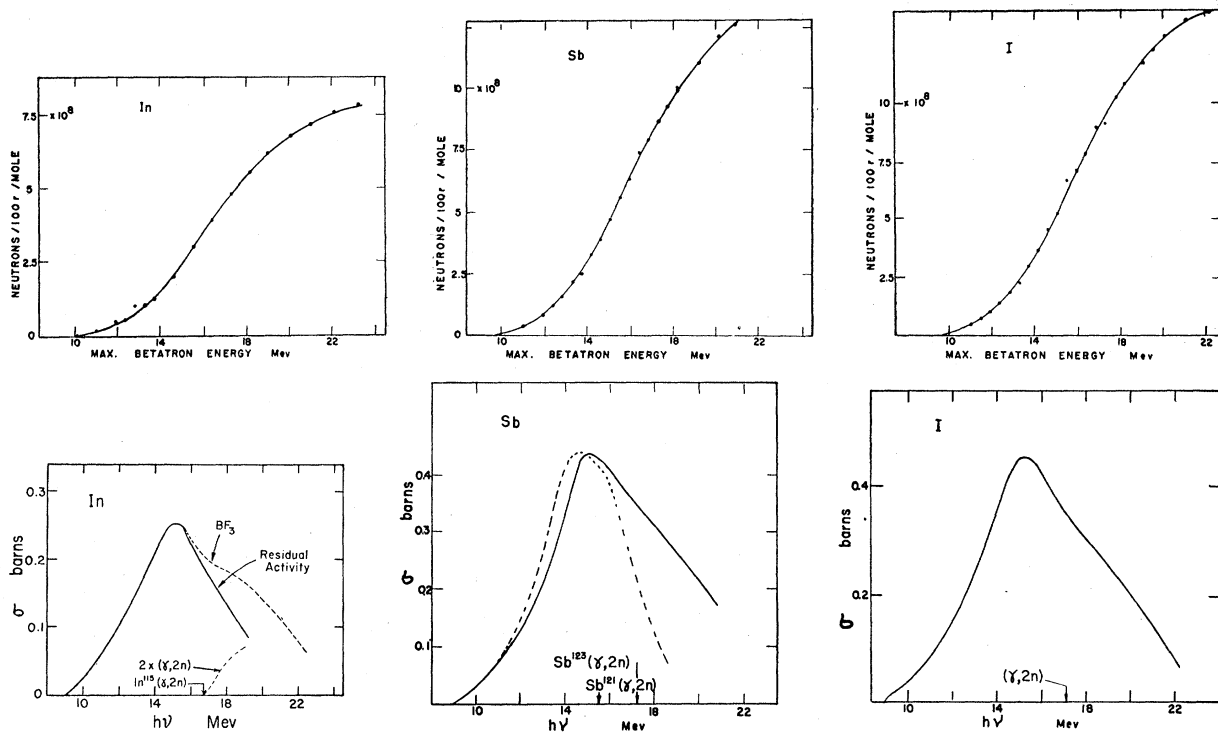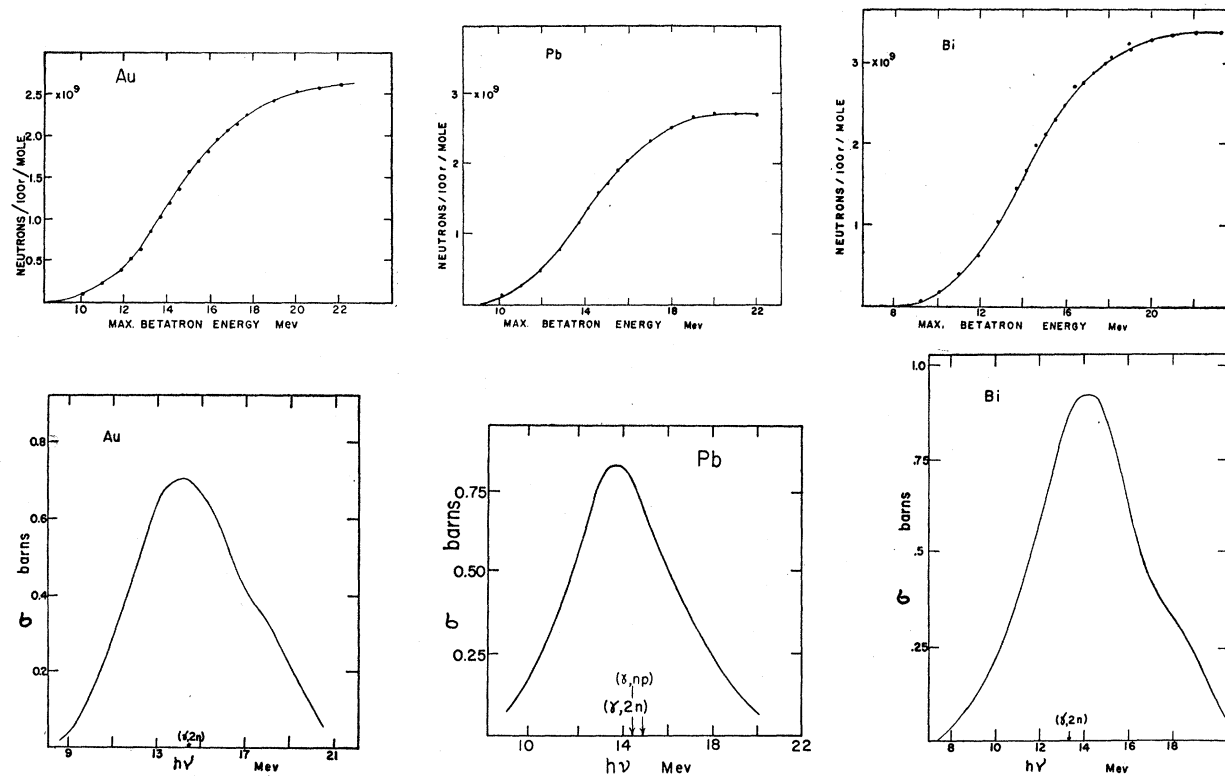
TABLE II. Characteristics of photonuclear cross sections.

Element	Half-width of σ (γ, n)	Half-width of σ for element	E_m (Mev)	σ_m (barns)	Integrated σ (Mev-barn) (γ, n)	(γ, p)	$(\gamma, 2n)$	$(\gamma, n)+(\gamma, np)$ $+2(\gamma, 2n)$	Ref.
Be⁹	4.7(γ, p)		22.2	0.0027		0.011			b
C		2.0	21.4	0.014	0.029				c
C¹²	2.8		22.9	0.013	0.046				d
C		1.7(γ, p)	21.5	0.034		0.063			e
N¹⁴			24.2	0.0028	0.015ᵃ				f
O			21.9	0.0089	0.019ᵃ				c
O¹⁶			24.2	0.011	0.031ᵃ				f
F¹⁹	~13		~20	0.0035	0.076		0.005		g
Na		6.0	18.3	0.013				0.081	c
Mg		3.9	18.8	0.011				0.048	c
Mg²⁴	5.8		19.4	0.0098	0.057				h
Mg²⁵⁺²⁶		~4.2	17.8	~0.016	~0.065				c
Mg²⁵	6.0(γ, p)		21.7	0.015		0.10			h
Mg²⁶	3.3(γ, p)		22.6	0.019		0.085			h
Al		4.0	19.7	0.023				0.10	c
Al²⁷	4.7		19.2	0.008	0.045				h
Al		5.4(γ, p)	21.2	0.022		0.12			e
Si²⁸	3.5		20.9	0.021	0.070				i
P		5.7	20.5	0.029	0.14		0.034(γ, np)	0.17	c
P³¹	6.5		19.5	0.017	0.13				j
P³¹			20	0.017	0.099		0.047(γ, np)	0.15	k
S		5.2	19.8	0.013				0.075	c
S³²	4.5		20.1	0.015	0.069				i
S³²	1.0(γ, d)		25.6	0.006			0.016(γ, d)		j, l
S³⁴	4		~17	~0.060				~0.20	c
Ca⁴⁰	4.2		19.3	0.015	0.065				i
Mn		>8	~19	0.10				~0.46ᵃ	c
Fe		6.1	18.0	0.075				0.47	c
Fe⁵⁴	6.3		18.7	0.067	0.48				d
Ni⁵⁸	5.6		18.5	0.054	0.34				d
Ni		5.4(γ, p)	18.7	0.058		0.32			e
Co		5.4	16.9	0.13				0.75	c
Co		5.7(γ, p)	21.5	0.024		0.14			e
Cu		7.1	19.5	0.12			0.054	0.87	c
Cu⁶³	6.1		18.1	0.10	0.66				d
Cu⁶⁵	7.0		18.6	0.15	1.11				d
Zn⁶⁴	7.9		18.7	0.12	0.99				d
As	~6.2	9.4	17	0.093	0.76		0.11	0.98	c
Br⁸⁰	8.0		18.0	0.13	1.08				m
Rb⁸⁷	6.0		17.5	0.23	1.68				n
Zr⁹⁰	5.7		18.0	0.27	1.67				n
Mo		6.1	15.7					1.62	c
Mo⁹²	6.0		18.7	0.14	0.85				n
Nb		6.1	17.3	0.26				1.71	c
Nb		6.6(γ, p)	21.3	0.018		0.12			e
Ag		9.2	16.3	0.20	2.1		0.22	2.5	c
Ag¹⁰⁹	4.6		16.5	0.32	1.65				o
In	~5.8	8.0	15.2	0.25	~1.6		~0.20	~2.0	c
In¹¹⁵	5.5		15.0	0.42	2.7				p
In¹¹⁵	~8(γ, γ')		~15	0.05				~0.4(γ, γ')	p
Sb		7.2	15.2	0.44				3.1	c
Sb¹²¹	4.8		14.8	0.68	3.5				d
Sb¹²³	4.8		14.8	0.36	1.9				d
I	~5.0	6.6	15.2	0.45				3.1	c
Ta¹⁸¹	4.6		13.9		>0.47				d
Au	~5.6	6.3	14.2	0.70				4.6	c
Au¹⁹⁷	~10(γ, γ')		15	>0.025				>0.25(γ, γ')	q
Pb		5.3	13.7	0.81				4.8	c
Pb²⁰⁷⁺²⁰⁸	~6.5(γ, p)		22.0	0.028		~0.17			r
Bi		5.4	14.2	0.92				4.1	c

ᵃ Integrated cross section to peak position.
ᵇ Haslam, Katz, Crosby, Summers-Gill, and Cameron, Can. J. Phys. 31, 210 (1953).
ᶜ Results from present experiments.
ᵈ See reference 24.
ᵉ See reference 34.
ᶠ Johns, Horsley, Haslam, and Quinton, Phys. Rev. 84, 856 (1951).
ᵍ Horsley, Haslam, and Johns, Phys. Rev. 87, 756 (1952).
ʰ See reference 22.
ⁱ Summers-Gill, Haslam, and Katz, Can. J. Phys. 31, 70 (1953).

ʲ See reference 25.
ᵏ See reference 23.
ˡ L. Katz and A. S. Penfold, Phys. Rev. 83, 169 (1951).
ᵐ Katz, Pease, and Moody, Can. J. Phys. 30, 476 (1952).
ⁿ Katz, Baker, and Montalbetti, Can. J. Phys. 31, 250 (1953).
ᵒ B. C. Diven and G. M. Almy, Phys. Rev. 80, 407 (1950).
ᵖ See reference 28.
�q A. G. W. Cameron and L. Katz, Phys. Rev. 84, 1264 (1951).
ʳ A. G. W. Cameron and L. Katz, Phys. Rev. 83, 1264 (1951).

followed by the usual resonance curve found previously[21] in residual activity measurements. As in the case of carbon, the activation curve obtained by residual activity in the present experiment differs considerably from that found previously, the general features of the cross-section curves are however not greatly altered.

Sodium (Na[24] 100 Percent, 12.1)

This is a new cross-section curve since it cannot be measured by residual activity. The (γ, np) threshold was calculated to be 19.2 Mev from the mass data of Li.[16] Thus the high-energy side of the curve may have a contribution from this reaction.

Magnesium (Mg[24] 78.6 Percent, 16.5; Mg[25] 10.1 Percent, 7.3; Mg[26] 11.3 Percent, 11.1)

The solid curve is the cross section for all of the magnesium isotopes. The (γ, n) cross section for the 79 percent isotope as measured by Katz and Cameron[19] is also shown (corrected for isotopic abundance). The difference in the low energy side between these curves may be attributed to the sum of the Mg[25](γ, n) and Mg[26](γ, n) reactions. It must be emphasized that since we are subtracting almost equal cross sections the upper part of the difference curve may be greatly in error. We should also note that a change of 20 percent in the residual activity curve would make it coincide with the BF$_3$ curve at the peak. This is within experimental accuracy.

Aluminum (Al[27] 100 Percent, 12.8)

The cross-section curve obtained here has the same relative shape as that of Katz and Cameron.[22] Its absolute magnitude is however greater by a factor of 3. There seems to be no reason for this larger discrepancy, it is believed however that the present measurements are more reliable. As previously discussed, the activation curves were standardized in one continuous run and all calculations were carried out in a standardized manner, considerably reducing the chance of relative errors. Good agreement is also obtained between the neutron yields in our activation curves at 18 and 22 Mev and those reported by Price and Kerst.[3]

Phosphorus (P[31] 100 Percent, 12.1)

Yield curves obtained by Halpern, Mann, and Nathans[23] from residual activity measurements and direct neutron detection are compared in Fig. 5 to those found by us. The curves have been arbitrarily normalized, at 18 Mev since Halpern et al. published only relative yields, and our neutron yield curve was somewhat higher at this point than the previous activation curve, though well within experimental accuracy. It will be seen that the shapes of the curves are in excellent

agreement below the normalization point, but at greater energies our yields are consistently higher.

The difference between the residual activity yield curve and the direct neutron detection yield above 18 Mev may be caused by the (γ, np) reaction whose threshold is 17.9 Mev. Both sets of data show this effect, with the percent contribution from the (γ, np) reaction being about the same in the two cases.

It would be tempting to attribute the difference between the results taken in the two laboratories to gamma-flux monitoring procedure, however the changes in the carbon and oxygen yield curves taken in our laboratory some three months apart would seem to rule this explanation out, since the same monitor was used in both cases.

An analysis of the "BF$_3$" yield curve by the photon difference method[24] gave the cross-section curve shown by the solid line of Fig. 5. The cross section for the (γ, n) reaction previously measured in this laboratory[25] was found to be about 15 percent lower at 18 Mev, well within experimental accuracy. If the two curves are then arbitrarily normalized at this energy, dashed curve of Fig. 5, then the difference is attributable to the (γ, np) reaction.

The area under the normalized (γ, n) curve gives an integrated cross section of 0.14 Mev-barn. The integrated cross section for the (γ, np) reaction is estimated to be 0.035 Mev-barn. These values are in fair agreement with those given by Halpern et al.,[23] namely 0.099 and 0.047 Mev-barn, respectively.

Sulfur (S[32] 95 Percent, 14.7; S[33] 0.74 Percent, 8.6; S[34] 4.2 Percent, 10.8; S[36] 0.016 Percent)

The S[32](γ, n)S[31] curve as measured by residual activity[26] was subtracted from the total neutron curve. The remaining portion may be attributed to the reaction in the S[34] isotope. Since this cross section is obtained by subtraction, it is obviously subject to a fairly large error in absolute value. Since S[34] is only a 4.2 percent isotope its cross section as given by these measurements is about 4 times that of S[32]. However, before comparing photon absorption cross sections account must be taken of the other modes of deexcitation, particularly (γ, p) which is quite threshold sensitive relative to (γ, n).

Manganese (Mn[55] 100 Percent, 10.0)

The total photoneutron cross-section curve (solid line) is much broader than expected from our knowledge of other (γ, n) reactions. In this region of the periodic table they are generally found to be 6 Mev wide at half-maximum. An assumed (γ, n) curve (6 Mev wide)

[21] Horsley, Haslam, and Johns, Can. J. Phys. 30, 159 (1952).
[22] L. Katz and A. G. W. Cameron, Phys. Rev. 84, 1115 (1951).
[23] Halpern, Mann, and Nathans, Phys. Rev. 88, 958 (1952).

[24] L. Katz and A. G. W. Cameron, Can. J. Phys. 29, 518 (1951).
[25] L. Katz and A. S. Penfold, Phys. Rev. 81, 815 (1951).
[26] The mass data of Li (see reference 16) gives a threshold for this reaction of 14.4 Mev. On the other hand, Haslam, Summers-Gill, and Crosby, (Can. J. Phys. 30, 257 (1952)) have measured this threshold at 15.0±0.1. We have taken the mean of the values.

has been drawn in as indicated by the dotted line. The difference is made up of twice the $(\gamma, 2n)$ reaction and the (γ, np) reaction. It is not possible to make a separation of the two latter reactions.

Iron (Fe^{54} 5.9 Percent, 13.8; Fe^{56} 91.6 Percent, 11.1; Fe^{57} 2.20 Percent, 7.7; Fe^{58} 0.33 Percent, 10.5)

By subtracting the (γ, n) cross section of the 6 percent isotope (dotted line) as measured by Katz et al.[27] from the total curve (solid line) the contributions from the remaining iron isotopes is obtained. Fe^{56} is the major isotope, so it forms the major portion of the total cross section curve. It is not possible to measure the (γ, n) reaction in this isotope by residual activities since the half-life of Fe^{55} is 4 years.

Cobalt (Co^{59} 100 Percent, 10.2)

Not very much can be said about this cross-section curve. When the (γ, n) cross section is determined by residual activity it will be possible to estimate the (γ, np) and $(\gamma, 2n)$ contributions.

Cooper (Cu^{63} 69.0 Percent, 10.9; Cu^{65} 31.0 Percent, 9.8)

Copper was taken as the standard to which all elements were normalized at 18 Mev. The residual activity cross-section curve shown in this figure was obtained by combining the Cu$^{63}(\gamma, n)$Cu^{62} and Cu$^{65}(\gamma, n)$-Cu^{64} cross sections according to their isotopic abundance. The shape of the experimental curve is in good agreement with that of residual activity measurements except beyond 18.5 Mev; the difference probably being the result of the $(\gamma, 2n)$ and (γ, np) reactions.

Zinc (Zn^{64} 48.9 Percent, 11.6; Zn^{66} 27.8 Percent, 11.1; Zn^{67} 4.1 Percent, 7.0; Zn^{68} 18.6 Percent, 10.1; Zn^{70} 0.63 Percent)

A detailed analysis to determine each cross curve cannot be made since there are four major isotopes. However, taking the difference between the total photoneutron cross-section curve and that obtained from residual activity for the Zn$^{64}(\gamma, n)$Zn^{63} reaction (properly corrected for isotopic abundance), the contribution from the remaining isotopes is obtained. The threshold for the $(\gamma, 2n)$ reaction in Zn^{64} is 21.6 Mev. The thresholds for the $(\gamma, 2n)$ reactions in the other isotopes are not known.

Arsenic (As^{75} 100 Percent, 10.1)

The shape of the cross-section curve is very odd. In fact it is rather obvious that it is made up of 2 curves, one for the (γ, n) and the other for the $(\gamma, 2n)$ reaction. An analysis of the contribution of $(\gamma, 2n)$ is given in the discussion.

Niobium (Nb^{93} 100 Percent, 8.7)

The cross-section curve exhibits the usual resonance characteristics. The $(\gamma, 2n)$ reaction is not as evident in this case as for example in arsenic.

Molybdenum (Mo^{92} 15.7 Percent, 13.1; Mo^{94} 9.3 Percent, Mo^{95} 15.7 Percent, Mo^{96} 16.5 Percent, Mo^{97} 9.5 Percent, Mo^{98} 23.9 Percent, Mo^{100} 9.5 Percent)

The large number of high percentage isotopes present in this element with widely different thresholds precludes an analysis of this curve.

Silver (Ag^{107} 51.4 Percent, 9.5; Ag^{109} 48.6 Percent, 9.0)

The total photoneutron cross section is extremely broad. Subtracting the (γ, n) curve as obtained by Almy and Diven[11] using the activity method, the resulting curve is likely attributable to the $(\gamma, 2n)$ process. Following Almy and Diven we assumed that the two isotopes of silver have the same shape since their thresholds are nearly equal.

Indium (In^{115} 95.8 Percent, 9.1; In^{113} 4.2 Percent, 9.7)

Here it seems very likely that the total curve is made up of two separate curves, one attributed to the (γ, n) process and the other to the $(\gamma, 2n)$ reaction. Recently Goldemberg and Katz[28] have measured by residual activity both the (γ, n) and the $(\gamma, 2n)$ reaction in In^{115} in this laboratory. Although the absolute cross sections which they found were somewhat larger (peak cross sections of 0.42 barn for the (γ, n) reaction and about 0.11 barn for the $(\gamma, 2n)$ reaction), the shapes of their curves are almost identical to those shown in the figure. The value reported here would be somewhat depressed, since indium acts as a neutron sink due to its large thermal neutron absorption cross section.

Antimony (Sb^{121} 57.2 Percent, 8.3; Sb^{123} 42.8 Percent, 9.3)

The solid line is the total cross section for all isotopes. The dotted line is that measured by Johns et al.[10] for Sb^{123} (43 percent isotope), and has not been corrected for isotopic abundance. This shows that the cross section curves for both isotopes must be very similar in shape. There is obviously a large contribution from the $(\gamma, 2n)$ reactions; the difference between the two curves is, however, not shown explicitly since the (γ, n) cross section in Sb^{121} is not known.

Iodine (I^{127} 100 Percent, 9.1)

This curve exhibits the usual characteristics of all other (γ, n) reactions. This cross section has as yet not been measured by residual activity.

[27] Katz, Johns, Baker, Haslam, and Douglas, Phys. Rev. 82, 271 (1951).

[28] J. Goldemberg and L. Katz, Phys. Rev. 90, 308 (1953).

Gold (Au[197] 100 Percent, 7.9)

The $(\gamma, 2n)$ reaction is not readily separated here, as no strong anomaly is present in the total cross section curve.

Lead (Pb[204] 1.3 Percent, 8.7; Pb[206] 26 Percent, 10.6; Pb[207] 21 Percent, 6.9; Pb[208] 52 Percent, 7.2)

Though there are several high percentage isotopes in lead, the rather smooth over-all cross-section curve is not unexpected since their (γ, n) thresholds are not too different.

Cameron, Harms, and Katz[29] have measured the cross sections for the reactions $Pb^{207}(\gamma, p)Tl^{206}$, $Pb^{208}(\gamma, p)Tl^{207}$ and $Pb^{208}(\gamma, d+np)Tl^{206}$ by detecting the activity of the residual nuclei. Since Tl^{206} and Tl^{207} have almost identical half-lives, the cross section for the individual reactions could not be separated. At 18 Mev, for example, they find the cross section to be about 1 mb, this value being almost wholly the result of the sum of the (γ, p) reactions.

The (γ, n) cross section at the same energy is about 100 mb. Thus we must conclude that at this energy $\sigma_{\gamma, p}/\sigma_{\gamma, n} \simeq 0.01$. On the basis of statistical theory this

TABLE III. Thresholds for the isotopes of lead.

Isotope	Threshold (Mev)			
	(γ, n)	(γ, p)	(γ, np)	$(\gamma, 2n)$
Pb[206]	10.6	7.1	14.3	14.5
Pb[207]	7.2	8.1	14.3	17.9
Pb[208]	6.9	8.4	15.0	14.2
Natural element (average)	7.9	7.9	14.5	14.9

is rather large considering the height of the potential barrier which the protons must overcome, but is of the correct order of magnitude for a direct photoproton effect. In order to compare this ratio with that predicted by statistical theory we must first calculate the thresholds for these reactions in the various isotopes. The results of such calculations using measured nuclear masses[17] are given in Table III. It will be seen that these are almost equal.

The average threshold (averaged according to isotopic abundance) is the same for (γ, p) and (γ, n) and the individual values do not deviate very far from these. Taking this average at $\simeq 8$ Mev, the theoretical ratio may be calculated. This ratio is precisely the ratio F_p/F_n at $\epsilon_{bY} = 10$ Mev given by Blatt and Weisskopf.[30] From their graphs we find $F_p/F_n \simeq 10^2/10^8 = 10^{-6}$. Thus the statistical ratio is much lower than that found experimentally; on the other hand there is ample evidence in the literature[11,31] for a small direct photoproton effect.

[29] Cameron, Harms, and Katz, Phys. Rev. 83, 1264 (1951).
[30] J. M. Blatt and V. F. Weisskopf, *Theoretical Nuclear Physics* (John Wiley and Sons, Inc., New York, 1952), p. 373.
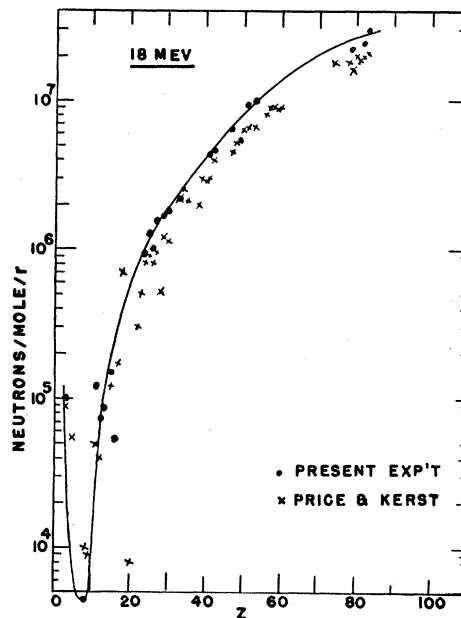[31] E. D. Courant, Phys. Rev. 82, 703 (1951).

FIG. 11. Neutron yields with betatron operating at 18 Mev compared to the data of Price and Kerst.

Bismuth (Bi[209] 100 Percent, 7.4)

This cross-section curve exhibits the anomaly on the high-energy side found by Halpern, Nathans, and Mann[6] and attributed by them to the $(\gamma, 2n)$ reaction. The two cross-section curves peak at about the same energy but ours is about twice as large. In view of the excellent agreement between the neutron yields meas-
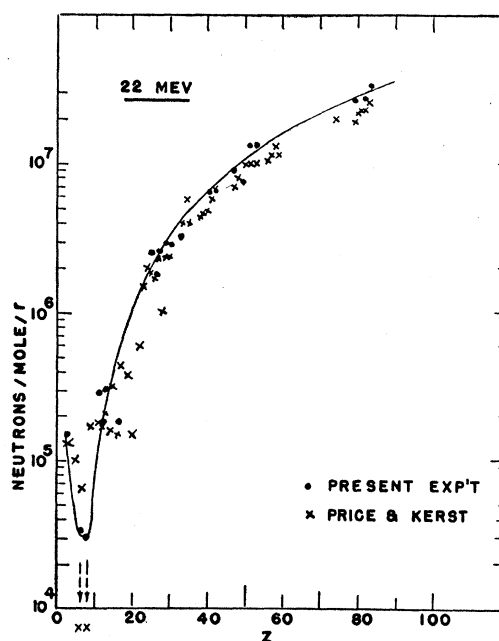

FIG. 12. Neutron yields with betatron operating at 22 Mev compared to the data of Price and Kerst.
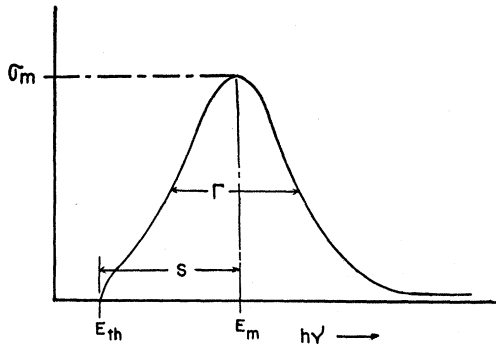
FIG. 13. Figure to illustrate the various parameters used in the discussion.

ured by us and those reported by Price and Kerst,[3] it is felt that the larger cross section is probably correct.

DISCUSSION

The neutron yields at 18 and 22 Mev have been plotted in Figs. 11 and 12, respectively, as functions of Z and are compared to the data of Price and Kerst. Our values are somewhat higher at both energies, though the difference is well within the combined experimental accuracy of both sets of data.

Very few detailed theoretical calculations of photonuclear intereactions have been attempted to date, except for the cases of light nuclei such as beryllium and deuterium. In fact, such calculations are at present not possible with any degree of assurance or accuracy. For this reason a discussion of the photoneutron systematics in the light of our measurements may be of interest to point the way to further research as well as perhaps inspire new theoretical analysis.

The various parameters which we will use to describe the photonuclear cross-section curves are illustrated in Fig. 13. The width Γ is defined by the following
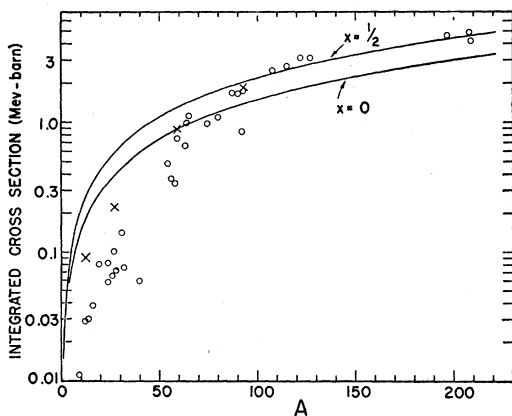

FIG. 14. Experimental values of the integrated cross sections given in Table II as a function of the mass number A. The contributions from the (γ, p) reactions in C^{12}, Al^{27}, Co^{59}, and Nb^{93} have been added in these elements and are shown by the crosses.

equation:

$$\sigma_m \Gamma = \int_0^\infty \sigma_c(\gamma) dE, \qquad (1)$$

where $\sigma_c(\gamma)$ is the cross section for photon capture by the nucleus, and σ_m is the peak cross section for photon absorption. The width Γ is not necessarily equal to the width at half-maximum because of the tail which extends to very high energies. The measurements of Terwilliger and of Jones have however shown that the area under this tail is a small fraction of the area under the giant resonance and for this reason it is expected that Γ is fairly proportional to the width at half-maximum. Terwilliger[4] points out that in the case of tantalum the integrated cross section is 4.20 Mev-barn under the resonance curve (0–27.5 Mev) and only 0.67 Mev-barn under the tail (27.5 to 65 Mev).
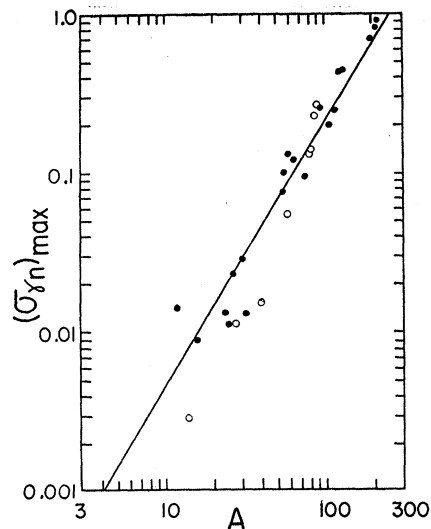

FIG. 15. Experimental values of the peak (γ, n) cross sections as a function of mass number A. The slope of the line shows that it varies as $A^{5/3}$.

The predicted value of the integrated cross section for all photonuclear reactions resulting from dipole photon absorption in a given isotope is, according to Levinger and Bethe,[32] given by the following equation;

$$\int_0^\infty \sigma_c(\gamma) dE = 0.015 A (1+0.8x), \qquad (2)$$

where A is the atomic weight, and x is the fraction of the neutron-proton force which is of exchange character. Interactions of other multipolarities were calculated by them and found to be negligible.

Values of the integrated cross sections listed in Table II are shown in Fig. 14. The values plotted are for the individual isotopes where those are given or the total cross section listed in column 9 for those elements

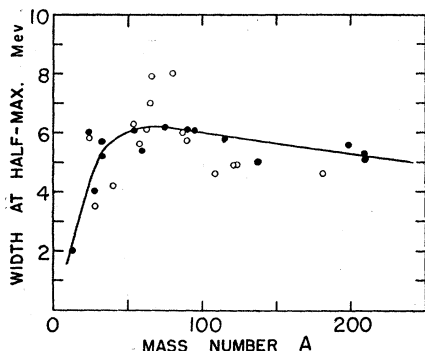[32] J. S. Levinger and H. A. Bethe, Phys. Rev. 78, 115 (1950).

FIG. 16. The measured widths at half cross-section width for the (γ, n) reactions as a function of mass number A.

which are predominantly composed of a single isotope. Since this total cross section contains contributions amounting to twice the $(\gamma, 2n)$ reaction then these points may be overestimated by as much as 10 percent. The two curves on this diagram represent Eq. (2) with $x=0$ and $x=\frac{1}{2}$. This latter value of x is indicated by the neutron-proton scattering experiments[33] of the Berkeley group.

The experimental points fall very close to the $x=\frac{1}{2}$ line for $A \geq 100$, but drop below both lines in the lighter elements. In this region the (γ, p) reactions are expected to be important because of the low Coulomb barrier.

Some (γ, p) reactions have been measured by Halpern and Mann.[34] Taking their results for C^{12}, Al^{27}, Co^{59}, and Nb^{93} (the last 3 being 100 percent isotopes and C^{12} a 99 percent isotope) and adding them to ours we find the sums in the two lighter elements are still below the $x=0$ line, that for Co^{59} falls on this line and that for Nb^{93} approaches the integrated cross section with $x=\frac{1}{2}$. These values are indicated by crosses on Fig. 15.

A plot of the peak values of the (γ, n) cross section $(\sigma_{\gamma, n})_m$ as a function of atomic number A is shown in Fig. 15. The straight line drawn through the points shows that $(\sigma_{\gamma, n})_m$ may be represented as a function of $A^{5/3}$, where the exponent is the slope of the line.

The widths of the cross-section curve at half-maximum were plotted as a function of A and are shown in Fig. 16. Beyond $A=50$ there is a definite trend to narrower widths with increasing A. Terwilliger[4] also came to the same conclusion, though somewhat indirectly. If we assume that Γ is proportional to the width at half-maximum of the photon absorption curve and that this in turn is proportional to the width of the (γ, n) curve, at least for the heavier nuclei then Γ also is a decreasing function of atomic number, changing from a relative value of 1 at $A\simeq50$ to 0.7 at $A\simeq200$.

A log-log plot of $E_{\max}$ as a function of mass number is shown in Fig. 17. The straight line drawn through

these points may be represented by the equation:

$$E_m = 37A^{-0.186}. \tag{3}$$

A similar equation was found by Katz and Cameron[24] to fit data obtained by residual activity. The exponent found by these authors is identical with that of the above equation. The constant preceding A was found by them to be 38.4 instead of 37. The newer results are believed to be more accurate. According to the theory of Goldhaber and Teller[35] one would expect the exponent to be 1/6; on the other hand the computations of Steinwedel, Jensen, and Jensen[36] predict an exponent of 1/3. Our results obviously favor the calculations of Goldhaber and Teller.‡

A similar log-log plot was made of the threshold energy against the mass number. This also is shown in Fig. 17. A best fit straight line drawn through these points is given by the equation:

$$E_{th} = 32A^{-0.270}. \tag{4}$$

The difference between these two equations $\bar{S}_n = E_m - E_{th}$, represents the mean distance between the peak of the photoneutron cross section and the threshold for the (γ, n) reaction. It is interesting to note that this distance is essentially constant, independent of mass number. Thus, according to the above two equations for $A=10$, we find $\bar{S}_n=7$ Mev and for $A=200$, $\bar{S}_n=6.2$ Mev.

Combining Eqs. (1) and (2) we find
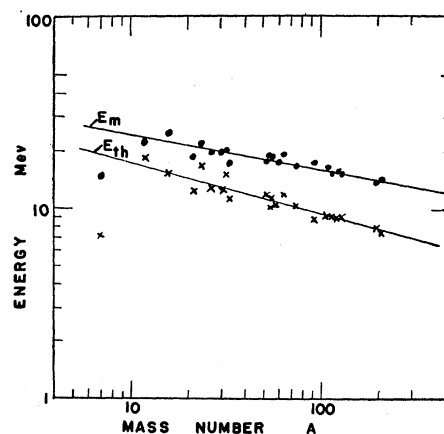
$$\sigma_m E_m = 0.015A(1+0.8x)E_m/\Gamma. \tag{5}$$

FIG. 17. Plot of E_m for the (γ, n) reaction as a function of mass number. It is well represented by the equation $E_m = 37A^{-0.186}$. The lower plot is that of the (γ, n) threshold in the same isotopes for which E_m is given. This line can be represented by $E_{th} = 32A^{-0.270}$. The distance between these lines is quite constant independent of A.

[35] M. Goldhaber and E. Teller, Phys. Rev. 74, 1046 (1948).
[36] Steinwedel, Jensen, and Jensen, Phys. Rev. 79, 1019 (1950).
‡ It is not possible to differentiate between these two exponents if only the measurements for nuclei with mass number greater than 100 are used.

[33] Hadley, Kelly, Leith, Segré, Wiegand, and York, Phys. Rev. 75, 351 (1949).
[34] J. Halpern and A. K. Mann, Phys. Rev. 83, 370 (1951).

Both E_m and Γ are decreasing functions of the mass number A, and the ratio E_m/Γ is quite independent of A for $A \geq 50$. Thus we conclude that

$$\sigma_m E_m \propto A \quad \text{for} \quad A \geq 50. \tag{6}$$

The variation of E_m with A, for the (γ, n) reaction only, is given by Eq. (3) and is probably the same for the photon capture cross section $\sigma_c(\gamma)$. In this case, combining (3) with Eq. (6) we find that σ_m should be expected to vary as $A^{1.186}$. In a recent paper Peaslee[37] has indicated that the peak cross section of the giant resonances should increase roughly with A throughout the periodic table.

In a few cases it was possible to determine unambiguously the $(\gamma, 2n)$ cross section from this experiment. From statistical theory[38] the ratio of $(\gamma, 2n)$ to (γ, n) is given as:

$$\frac{\sigma_{(\gamma, 2n)}}{\sigma_{(\gamma, n)}} = 1 - \left[1 + \left(\frac{a}{E} \right)^{\frac{1}{2}} (E - E_b) \right]$$

$$\times \exp\left[-\left(\frac{a}{E} \right)^{\frac{1}{2}} (E - E_b) \right],$$

where a is a constant for a given A, E is the photon energy less the threshold energy for the (γ, n) reaction, and E_b is the threshold energy for the $(\gamma, 2n)$ reaction less the threshold energy for the (γ, n) reaction. The cross section has been calculated using this equation for indium and arsenic with the values of a taken from

[37] D. C. Peaslee, Phys. Rev. **88**, 812 (1952).

[38] Feld, Feshbach, Goldhaber, Goldstein, and Weisskopf, Final Report of the Fast Neutron Data Project, U. S. Atomic Energy Commission NYO-636, January 1951 (unpublished).

TABLE IV. Measured ratio of $\sigma_{(\gamma, 2n)}/\sigma_{(\gamma, n)}$ compared to that calculated from statistical theory.

Photon energy (Mev)	$\sigma_{(\gamma, 2n)}/\sigma_{(\gamma, n)}$	
	Calculated	Experimental
	Indium	
17	0.12	0.17
18	0.35	0.34
19	0.52	0.8
	Arsenic	
18	0.19	0.15
19	0.40	0.33
20	0.53	0.69
21	0.64	0.90

Blatt and Weisskopf[28] and are compared ot the experimental results in Table IV.

Considering the difficulty in separating the $(\gamma, 2n)$ cross section accurately from the total cross-section curve the agreement is very good.

In the heavy elements (beyond indium) it was not possible to determine the amount of $(\gamma, 2n)$ present. However when information becomes available on the (γ, n) cross section in heavy nuclei it will be possible to obtain the $(\gamma, 2n)$ contribution. The 100 percent isotopes, iodine, gold, and bismuth should give this contribution with the least ambiguity.

The integrated cross section for the $(\gamma, 2n)$ reaction was determined to be the order of 10 percent of the integrated cross section for the (γ, n) reaction.

The authors would like to thank Dr. A. G. W. Cameron for his assistance during the initial phases of this work and Dr. P. A. Forsyth for his help with some of the circuitry design problems.